2-12-2015

Vascular endothelial growth factor receptor 3 signaling contributes to angioobliterative pulmonary hypertension

Ayser Al-Husseini
Virginia Commonwealth University

Donatas Kraskauskas
Virginia Commonwealth University

Eleanora Mezzaroma
Virginia Commonwealth University

Andrea Nordio
Virginia Commonwealth University

Daniela Farkas
Virginia Commonwealth University

See next page for additional authors

Vascular endothelial growth factor receptor 3 signaling contributes to angioobliterative pulmonary hypertension

Ayser Al-Husseini,[1] Donatas Kraskauskas,[1] Eleanora Mezzaroma,[2] Andrea Nordio,[2] Daniela Farkas,[1] Jennifer I. Drake,[1] Antonio Abbate,[2] Quentin Felty,[3] Norbert F. Voelkel[1]

[1]Victoria Johnson Laboratory for Lung Research, Virginia Commonwealth University, Richmond, Virginia, USA; [2]VCU Pauley Heart Center, Virginia Commonwealth University, Richmond, Virginia, USA; [3]Department of Environmental and Occupational Health, Florida International University, Miami, Florida, USA

Abstract: The mechanisms involved in the development of severe angioobliterative pulmonary arterial hypertension (PAH) are multicellular and complex. Many of the features of human severe PAH, including angioobliteration, lung perivascular inflammation, and right heart failure, are reproduced in the Sugen 5416/chronic hypoxia (SuHx) rat model. Here we address, at first glance, the confusing and paradoxical aspect of the model, namely, that treatment of rats with the antiangiogenic vascular endothelial growth factor (VEGF) receptor 1 and 2 kinase inhibitor, Sugen 5416, when combined with chronic hypoxia, causes angioproliferative pulmonary vascular disease. We postulated that signaling through the unblocked VEGF receptor VEGFR3 (or flt4) could account for some of the pulmonary arteriolar lumen–occluding cell growth. We also considered that Sugen 5416–induced VEGFR1 and VEGFR2 blockade could alter the expression pattern of VEGF isoform proteins. Indeed, in the lungs of SuHx rats we found increased expression of the ligand proteins VEGF-C and VEGF-D as well as enhanced expression of the VEGFR3 protein. In contrast, in the failing right ventricle of SuHx rats there was a profound decrease in the expression of VEGF-B and VEGF-D in addition to the previously described reduction in VEGF-A expression. MAZ51, an inhibitor of VEGFR3 phosphorylation and VEGFR3 signaling, largely prevented the development of angioobliteration in the SuHx model; however, obliterated vessels did not reopen when animals with established PAH were treated with the VEGFR3 inhibitor. Part of the mechanism of vasoobliteration in the SuHx model occurs via VEGFR3. VEGFR1/VEGFR2 inhibition can be initially antiangiogenic by inducing lung vessel endothelial cell apoptosis; however, it can be subsequently angiogenic via VEGF-C and VEGF-D signaling through VEGFR3.

Keywords: Sugen 5416, chronic hypoxia, VEGF isoforms, VEGF receptor 3, sFlt-1, MAZ51, right heart failure, capillary rarefaction.

Pulm Circ 2015;5(1):101-116. DOI: 10.1086/679704.

INTRODUCTION

It is now well recognized that the pathobiology of severe forms of pulmonary arterial hypertension (PAH) is driven by a process that is multicellular and highly complex.[1] Resident lung vascular cells, inflammatory cells and cells of the immune system, bone marrow–derived cells, and various precursor or stem cells are all potential participants in the sequence of events leading to vascular remodeling; their particular and interactive roles in pulmonary vascular remodeling are under active investigation in a number of experimental models of PAH.[2-6] The concepts of apoptosis resistance of proliferating vascular cells[1,7] and of misguided angiogenesis have now advanced the field, and we have proposed that angioobliterative PAH is initiated by pulmonary vascular endothelial cell apoptosis. However, by itself endothelial cell apoptosis is insufficient to cause severe PAH. Instead, apoptosis-resistant cells emerge and proliferate, ultimately leading to vessel lumen obliteration,[1] perhaps aided by the weakening of a bone morphogenetic protein receptor type 2–dependent homeostatic control of pulmonary arteriolar wall injury-repair mechanisms.[8]

To investigate these mechanisms of lung vessel injury and repair, rat models of severe angioobliterative PAH and right heart failure,[9,10] which are based on chronic hyp-

Address correspondence to Dr. Norbert F. Voelkel, 1220 East Broad Street, Molecular Medicine Research Building, Room 6052, Richmond, VA 23298, USA. E-mail: nfvoelkel@gmail.com.

Submitted January 7, 2014; Accepted October 13, 2014; Electronically published February 12, 2015.

oxic exposure[11] or immunoinsufficiency[5] together—and very paradoxically—with the administration of an antiangiogenic vascular endothelial growth factor (VEGF) inhibitor, are now being examined.[8,12]

This apparent paradox of antiangiogenic drug–induced PAH can now be explained by taking into account an improved understanding of the role played by VEGF in vascular biology[13-15] and of the mechanisms of resistance of tumor cells to antiangiogenic drugs.[16,17] Collectively, a large number of new studies illustrate the multitude of biological effects that are attributable to VEGF-A, its various splice variants, and signals transmitted via several membrane and nuclear VEGF receptors.[18-24]

Although it has been shown that the potent endothelial cell growth factor VEGF and its receptor VEGFR2 (KDR) are highly expressed in lung vascular lesions of patients with idiopathic PAH (IPAH),[25] it remains unclear whether and how VEGF actually drives pulmonary angioproliferation in severe forms of human PAH. Certainly, the presence of elements that may participate in the pathobiological processes can be demonstrated by examining tissue samples from IPAH patients. However, such studies cannot explain disease mechanisms; thus, these studies need to be complemented by the interrogation of animal models of PAH.

To begin this interrogation, we here examine the Sugen 5416/chronic hypoxia (SuHx) rat model of severe angioobliterative PAH and address the question whether VEGF, in spite of the blockade of the receptors VEGFR1 and VEGFR2 by Sugen 5416, contributes to the pathogenesis of PAH in this model. Because Sugen 5416 inhibits the intracellular VEGFRI and VEGFRII tyrosine kinases, we wondered whether the lymphangiogenic and angiogenic VEGFR3 and its ligands VEGF-C and VEGF-D[26-31] are expressed in the lungs of animals with PAH and whether the VEGFR3 blocker MAZ51[32,33] ameliorates the development of severe PAH in SuHx animals.

Our experiments show that a change in the VEGF isoform and VEGF receptor expression pattern occurs in the lungs and hearts of SuHx-treated pulmonary hypertensive rats and that signaling via the overexpressed VEGFR3 (flt4) contributes to the development of angioobliterative PAH. In the SuHx rat model, severe PAH is associated with right heart failure[34] and, in contrast to the cell proliferation that occludes the lung vessels, there is a right ventricular loss of microvessels, or capillary rarefaction. We have reported that this right ventricle (RV) capillary rarefaction is associated with a decreased myocardial expression of VEGF-A.[35] Now we show that the expression of the VEGF-B splice variant[36-38] is likewise decreased in the tissues of failing rat RVs, further supporting the hypothesis that loss of expression of angiogenesis factors can explain the capillary rarefaction[35,39] in failing RVs.[34]

METHODS

Animal models

All experiments were approved by the Institutional Animal Care and Use Committee of Virginia Commonwealth University. Pulmonary hypertension was induced in male Sprague-Dawley rats (body weight, 250 g) as follows: the animals received a single subcutaneous injection of the VEGF receptor tyrosine kinase inhibitor (Sugen 5416, 20 mg/kg) and were exposed to chronic hypoxia for 4 weeks (SuHx model), as described elsewhere.[11] Age- and sex-matched rats were exposed to 10% hypoxia for 4 weeks in the prevention studies and for 4 weeks followed by a return to room air for 2 weeks in the intervention studies. For hypoxia-only and control animals, age- and sex-matched rats were placed in the hypoxic chambers at room air, consecutively, for the same period of time as the other groups. MAZ51 (8 mg/kg; purchased from Calbiochem/EMD Millipore, San Diego, CA; 676492-10MG) was dissolved in carboxymethyl cellulose and administered subcutaneously every other day for 21 days.[32] At the end of the exposure period, each rat was anesthetized with an intramuscular injection of ketamine/xylazine. The thoracic cavities were opened by midline incision, and hemodynamic measurements were obtained using a 4.5-mm conductance catheter (Millar Instruments, Houston, TX) and the PowerLab data acquisition system (AD Instruments, Colorado Springs, CO). The right lung was removed and frozen in liquid nitrogen. The left lung was inflated with 0.5% low-melting agarose at a constant pressure of 25 cm of H_2O, fixed in 10% formalin for 48 hours, and used for immunohistochemistry (IHC) analysis. Right ventricular hypertrophy was measured as the ratio of right ventricular weight to left ventricular plus septal weight (RV/LV+S).

Antibodies and enzyme-linked immunosorbent assay (ELISA)

We used the following antibodies: rabbit anti-VEGF-A, rabbit anti-VEGF-D, mouse anti-SPARC (Santa Cruz Biotechnology, Santa Cruz, CA), rabbit anti-VEGF-B, goat anti-VEGFR2 (Abcam, Cambridge, United Kingdom), rabbit anti-VEGF-C, rabbit anti-VEGFR3 (Novus Biologicals, Littleton, CO), rabbit anti-tubulin (Cell Signaling, Beverly, MA), and mouse anti-β-actin (Sigma, St. Louis, MO). The ELISA for measuring rat sFlt-1 was purchased from Mybiosource (San Diego, CA; MBS007319).

Western blot analysis

Whole-cell lysate from one lobe of the right lung was prepared using radioimmunoprecipitation assay buffer (Sigma), and the protein concentration was determined using the Bio-Rad Protein DC Protein Assay (Bio-Rad, Hercules, CA). Whole cellular protein (35 μg/lane) was separated by sodium dodecyl sulfate (SDS) polyacrylamide gel electrophoresis with 4%–12% Bis-Tris Nupage gel (2-(N-morpholino) ethanesulfonic acid [MES] SDS running buffer) and blotted onto a polyvinylidene difluoride membrane. The membrane was incubated with blocking buffer (5% nonfat dry milk/phosphate-buffered saline [PBS] 0.1% Tween 20) at room temperature for 1 hour. Overnight at 4°C the membrane was then probed with the primary antibodies diluted in blocking buffer. Subsequently, membranes were incubated with horseradish peroxidase–conjugated anti-mouse or anti-rabbit antibody diluted 1 : 5000 in blocking buffer. Blots were developed with enhanced chemiluminescence (PerkinElmer, Waltham, MA) on GeneMate Blue Basic Autorad Films (BioExpress, Kaysville, UT). Blots were scanned and densitometry analysis was performed using ImageJ (National Institutes of Health, Bethesda, MD; http://imagej.nih.gov/ij/).

Statistical analysis

Data are presented as mean ± SEM. Two groups were compared with the two-tailed unpaired Student's *t* test, and more than two groups were compared with one-way analysis of variance followed by the Neuman-Keuls multiple comparison test. Statistical tests were performed and graphs were created with GraphPad Prism (ver. 5.0; GraphPad Software, San Diego, CA). Differences with $P < 0.05$ were considered significant.

Histology and microscopy

Lung tissue sections (4-μm paraffin sections) were used for staining; slides were incubated overnight with anti-VEGF-C rabbit antibody (1 : 50 dilution) and anti-VEGFR3 rabbit antibody (1 : 50 dilution). For counting the number of VEGFR3$^+$ luminal vascular cells, 10 random pulmonary arteries per tissue section stained with the anti-VEGFR3 antibody were captured at ×40 magnification, and then the number of VEGFR3$^+$ cells in the lumen of pulmonary vessels was counted.

For immunofluorescence (IF) and IHC stainings, 3-μm sections were rehydrated, which was followed by antigen retrieval with heat in citrate buffer (pH 6.0) for 20 min. Then, sections were blocked with 1% normal sheep serum (NSS)/PBS for 15 min and incubated with primary antibody 1 in 1% NSS in PBS overnight at 4°C. Sections were then incubated with secondary antibody 1 in PBS for 4 hours. For double IF staining, additional sequential incubations were performed with primary and secondary antibody 2 similar to 1. Finally, the sections were counterstained with 4′,6-diamidino-2-phenylindole (DAPI) at 1 : 20,000 for 5 minutes and mounted in SlowFade Gold (both Life Technologies/Invitrogen, Carlsbad, CA). For all IHC and IF stainings, controls with unspecific immunoglobulin G were run in parallel with each staining batch and treatment group.

Assessment of angioproliferative vascular lesions, perivascular inflammation, and the bronchus-associated lymphoid tissue (BALT) area

A quantitative analysis of luminal obstruction was conducted first by taking 10 random images per lung section from each rat and then counting the small pulmonary arteries (external diameter, <50 um), performed by two investigators blinded to treatment group. Vessels were assessed to grade for angioobliteration from two random left lung slices: no evidence of angioproliferation (open), partially obliterated (<50%), and full-luminal occlusion (obliterated).

For the purpose of assessing perivascular inflammation, fields were selected as described for the determination of the number of obliterated vessels. The perivascular infiltrate surrounding each pulmonary artery was quantified as follows: 0: absent, 1: minimal with a single layer clustering of inflammatory cells; 2: moderate, with localized clustering of inflammatory cells; and 3: abundant, with large clusters of inflammatory cells extending from the perivascular region toward adjacent alveoli. The final inflammatory score was the result of the following: [0 × *n* vessels with 0 score + 1 × *n* vessels with score of 1 + 2 × *n* vessels with score of 2 + 3 × *n* vessels with score of 3]/number of analyzed vessels, as described elsewhere;[40] 100 ± 36 vessels were examined per lung.

The BALT area was measured by analyzing 10 sections per group using AxioVision software (Zeiss, Oberkochen, Germany); an outline was drawn by manual placement and measured by planimetry.

RNA isolation

Total RNA was isolated from ~30 mg of snap-frozen rat heart and lung tissue using the Qiagen RNeasy Mini Kit (Qiagen, Valencia, CA). Tissues were homogenized with Buffer RLT and β-mercaptoethanol in an MP FastPrep-24 Lysing Matrix D tube (MP Biomedicals, Solon, OH), and RNA was isolated and purified in accordance with the manufacturer's protocol. Concentration of RNA was

calculated with a NanoDrop ND-1000 spectrophotometer (Thermo Fisher Scientific, Wilmington, DE). All samples had an A_{260}/A_{280} ratio between 1.9 and 2.1.

Microarray analysis

The amplification and hybridization process was as follows: 500 ng of total RNA was amplified and labeled with cyanine 5 (Cy5) and 500 ng of universal rat reference RNA (Stratagene, Santa Clara, CA) was amplified and labeled with cyanine 3 (Cy3) using the Agilent QuickAmp Labeling Kit (Agilent Technologies, Santa Clara, CA) to produce labeled complementary RNA (cRNA) in accordance with the manufacturer's protocol. After amplification and labeling, the dye incorporation was determined with a NanoDrop ND-1000 spectrophotometer (Thermo Fisher Scientific). All ratios were >8.0 pmol dye/μg cRNA, per the manufacturer's recommendation. We combined 825 ng of sample and 825 ng of reference RNA and incubated that with an Agilent whole-rat genome 4 $\times$ 44k microarray slide (Agilent Technologies, Wilmington, DE) for 17 hours at 65°C. After hybridization, slides were washed in accordance with the manufacturer's protocol and scanned with an Axon GenePix 4200A scanner (Axon Instruments, Union City, CA) at a resolution of 5 μM.

Raw expression data files were uploaded into R (R Development Core Team, Vienna, Austria) and normalized with the marray package[41] by means of the Lowess normalization algorithm and then exported to BRB-ArrayTools. Lowess intensity-dependent normalization was used to adjust for differences in labeling intensities of the Cy3 and Cy5 dyes. The adjusting factor varied over intensity levels.[42] Statistical analysis of biological replicates was performed using the significance analysis of microarrays algorithm[43] with a two-class paired-unpaired design (control lung vs. SuHx lung) and median centering to identify differentially expressed genes. The Δ value was chosen to give an acceptable false discovery rate of <5%.

VEGF polymerase chain reaction (PCR) array

Rat VEGF RT2 Profiler PCR Arrays were used to analyze gene expression changes. Arrays and RT2 Real-Time SyBR Green/ROX PCR Mix were purchased from SuperArray Bioscience (Frederick, MD). PCR was performed on a Stratagene Mx3000P instrument (Stratagene, La Jolla, CA), in accordance with the manufacturer's instructions. Lung samples from two normal and two SuHx rats were compared. For data analysis, the $\Delta\Delta$Ct method was used with the aid of a Microsoft Excel spreadsheet containing algorithms provided by the manufacturer. Fold changes were then calculated and reported as the SuHx/normal ratio for each tissue type.

RESULTS

Survey of expressed VEGF isoforms and VEGF receptors in lung and heart tissues

Because treatment of rats with the VEGFR1 and VEGFR2 receptor blocker combined with chronic hypoxia generates angioobliterative PAH that is associated with accumulation of inflammatory cells, activation of inflammatory cells in the lungs, and activation of inflammatory eicosanoid mediator–generating pathways,[44] we postulated that the tissue expression profile of VEGF isoforms and/or VEGF receptors would be altered because of inflammation or as a consequence of chronic VEGF receptor blockade. Lung tissue samples harvested from SuHx rats 4 weeks after the initiation of the experimental protocol were surveyed, and the expression of VEGF ligand isoforms was assessed by Western blotting. Although there was no significant change in the amount of VEGF-A and VEGF-B expression, VEGF-C and VEGF-D expression was increased; there was also a clear increase in expression of the VEGFR3 protein (Fig. 1*A*–1*F*). Figure 1*H* and 1*J* shows protein expression levels measured by ELISA of the antiangiogenic sFlt-1 in the lungs and serum, respectively, in which we found a significant reduction in lung tissue samples from SuHx rats and a trend toward an increase in serum from SuHx rats versus controls that did not reach statistical significance.

To contrast the lung tissue expression with the expression profile of the dysfunctional RV, we assessed protein expression in RV tissue samples from SuHx rats, again using Western blotting. We found a significant reduction in the expressed VEGF-A protein, confirming previous results.[35] A new finding was a reduction in the expressed VEGF-B and VEGF-D proteins, which was not shared by the RV tissues obtained from chronically hypoxic rats, while the expression of VEGF-C trended toward a decrease in the RV tissue samples from SuHx rats without reaching statistical significance (Fig. 2*A*–2*E*). With IHC staining, a clear reduction in VEGF-C from RV tissue of SuHx compared with control rats was observed (Fig. 2*F*). As for serum samples from SuHx rats, the antiangiogenic sFlt-1 trended toward an increase in RV tissue samples compared with control animals (Fig. 2*G*).

To corroborate the tissue expression and localize the expressed ligand and receptor proteins, we restricted the remainder of our investigation to examine VEGF-C and VEGFR3 expression in lung tissue samples. We found expression of VEGF-C in bronchial epithelium of normal rat lungs (Fig. 3*A*) but not in vascular endothelial cells. In contrast, VEGF-C was expressed in endothelial cells of muscularized pulmonary arterioles from SuHx rats (Fig. 3*A*). The VEGFR3 protein was highly expressed in

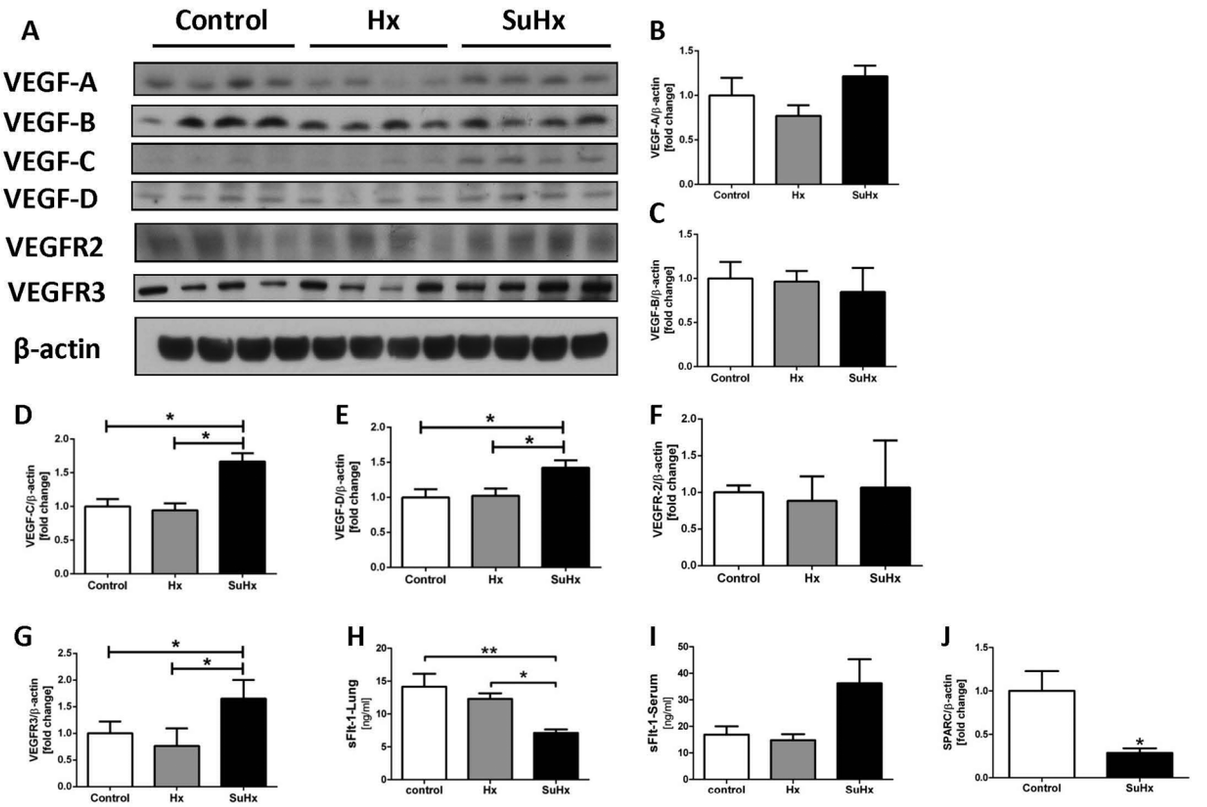

Figure 1. *A*, Lung tissue expression of the vascular endothelial growth factor (VEGF) isoform and of VEGF receptor proteins by Western blot analysis. There is no change in the expression of VEGF-A and VEGF-B proteins, while VEGF-C and VEGF-D are increased in expression in Sugen 5416/chronic hypoxia (SuHx) animals (*B–E*). VEGFR3 protein expression is increased when referenced to β-actin (*G*). The concentration of soluble VEGFR1 (sFlt-1) in the lung tissue is reduced (*H*), while the sFlt-1 levels trended toward an increase in the serum of SuHx animals (*I*). SPARC protein expression is reduced in whole-lung tissue protein extracts from SuHx rats (*J*). Asterisks indicate $P < 0.05$. $n = 4$. Hx: hypoxia-only rats.

cells of the lymph follicles (Fig. 3*B*) and in some of the vascular endothelial cells from normal lungs, hypoxic lungs, and SuHx lungs (Fig. 3*A*). In SuHx lungs, the cells surrounding vessel obliterating lesions and alveolar septal endothelial cells expressed VEGFR3 (Fig. 3*A*). Many of the lumen-obliterating cells stained highly positive 3 weeks after the start of the SuHx protocol.

We quantified VEGFR3$^+$ cells in and around the pulmonary vessels in the lungs of SuHx rats and found that the number of VEGFR3$^+$ cells had more than doubled by week 3 of the experimental protocol, while the number of VEGFR3$^+$ lumen-obliterating cells was increased at 3 weeks but not at 6 weeks (Fig. 3*C*). The reason why VEGFR3 expression of lumen-obliterating cells is transient is not clear.

To show coexpression of VEGFR3 with the endothelial cell marker (von Willebrand factor [vWF]), double immunofluorescence staining of VEGFR3 and vWF was done for the lung tissue sections of control, hypoxia, and SuHx rats (Fig. 4). There were VEFR3$^+$ cells in and around the lesions. In addition, there were several intimal, lumen-facing cells that express VEGFR3 but do not express vWF. In larger control vessels we saw some orange cells, indicating that in large vessels there are some VEGFR3$^+$ endothelial cells, and we speculate that these are precursor/stem cells.

Microarray expression pattern of genes encoding components of VEGF signal transduction in the lungs of SuHx animals

The microarray gene expression pattern for normal lungs and SuHx lungs (the animals had been killed at the end of the Sugen plus 4-week hypoxic exposure) was analyzed using published methodology[45] and was focused on genes encoding proteins involved in VEGF signaling, angiogenesis, and cell proliferation. Expressed genes were ranked according to their fold change compared with the expression observed in normoxic lungs. The gene encoding phospholipase D (PLD) was 4.8-fold overexpressed, that encoding early growth response 1 (Egr1) was 3.5-fold overexpressed,

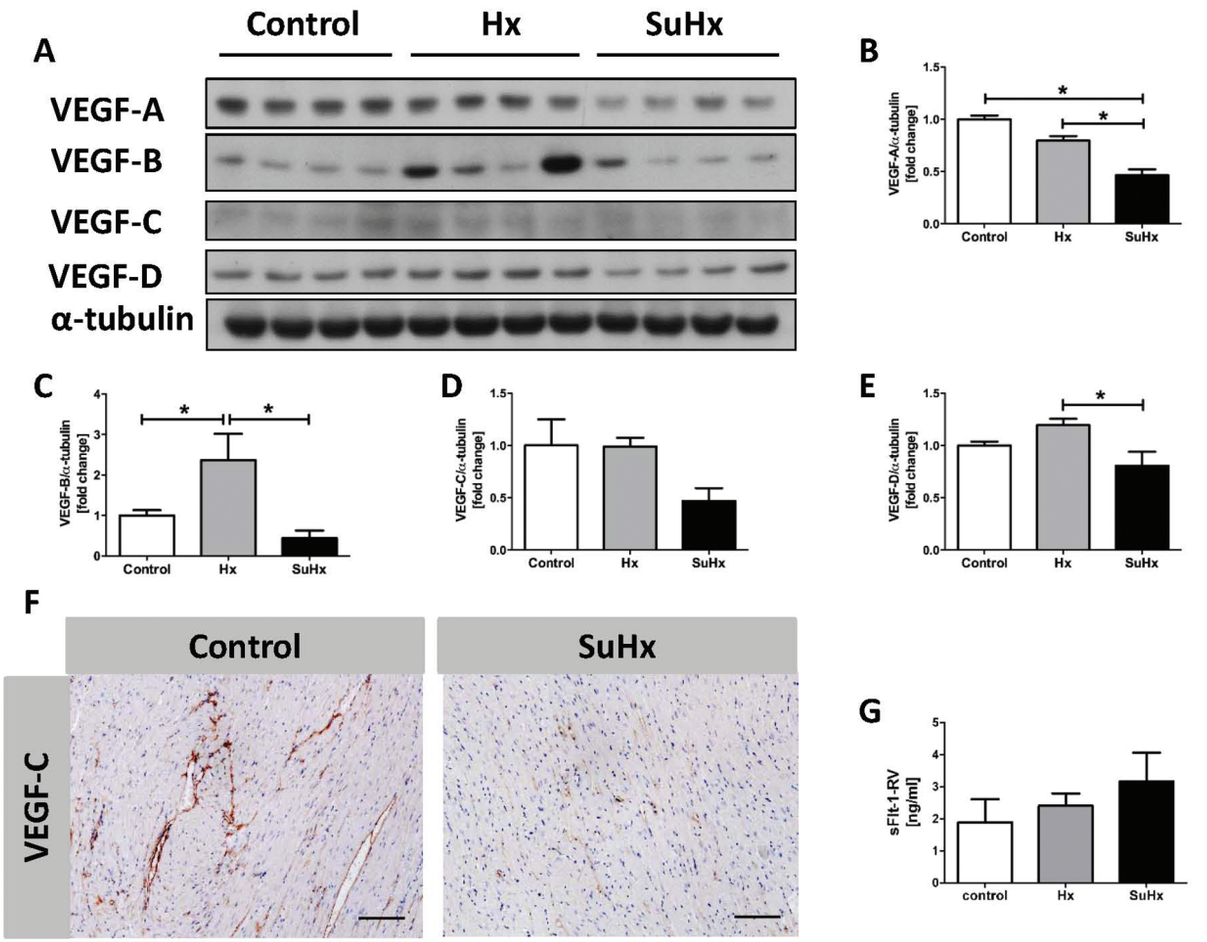

Figure 2. Proteins expressed in right ventricle (RV) tissues. All vascular endothelial growth factor (VEGF) isoform proteins are reduced in expression in the RV of Sugen 5416/chronic hypoxia (SuHx) rats (*A–E*). Immunohistochemistry (magnification, ×10; scale = 50 μm) shows loss of staining in the SuHx RV tissues when applying an antibody specifically directed against VEGF-C (*F*). There is only a trend toward an increased concentration of the sFlt-1 protein in the SuHx RV. Asterisks indicate $P < 0.05$. $n = 4$. Hx: hypoxia-only rats.

that encoding endothelial cell nitric oxide synthase (eNOS) was 2.6-fold overexpressed, and that encoding lysosomal-associated membrane protein 3 (Lamp3) was 5.7-fold overexpressed, while the gene encoding VEGFR2 showed significantly reduced expression (0.15), and SPARC (secreted protein, acidic, and rich in cysteine, also known as osteonectin) expression was also reduced (0.26; Table 1). We believe that these highly significant expression changes are of importance in the context of angiogenesis and lung vascular cell growth. It has been reported that VEGF stimulates PLD in endothelial cells via phospholipase C,[46] and pertinently PLD and VEGFR2 are colocalized in endothelial cell caveolae.[47] Lamp3 was originally isolated from lung tissue,[48] and it is overexpressed in several cancers.[49] Lamp3 is localized to endothelial Weibel-Palade bodies,[50] and its expression is increased by hypoxia.[51]

We confirmed the decreased expression of SPARC in SuHx lungs by measuring lung tissue SPARC protein expression (Fig. 1*J*). Kupprion et al.[52] have shown that SPARC inhibits the mitogenic effect of VEGF in microvascular endothelial cells, and there are multiple interactions between SPARC and VEGF signaling;[53,54] SPARC is induced by VEGF in vascular endothelial cells[55] and affects wound healing in a cell type–specific fashion.[56]

Treatment of SuHx rats with the VEGFR3 inhibitor MAZ51 ameliorates the severity of pulmonary hypertension and partially prevents lumen obliteration

Treatment of SuHx rats with every-other-day dosing of MAZ51 reduced right ventricular systolic pressure (RVSP) without affecting RV hypertrophy (Fig. 5*A*, 5*B*). However, the number of fully obliterated pulmonary arterioles was

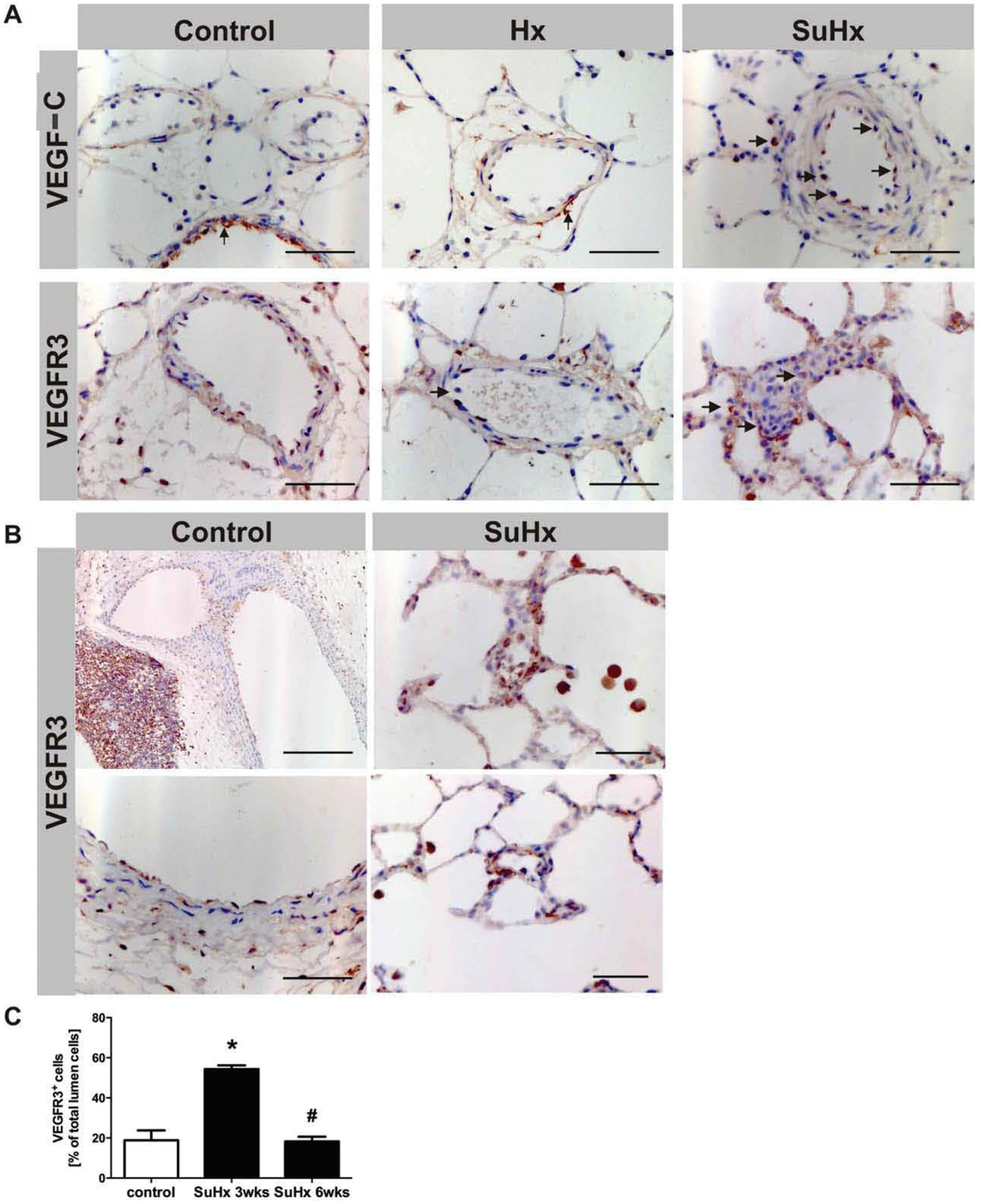

Figure 3. Immunohistochemistry of lung tissue sections (magnification, ×40; scale = 20 μm). Vascular endothelial growth factor (VEGF)–C protein is expressed in bronchial epithelium in normal control lungs; in lungs of chronically hypoxic rats there is faint staining of some cells of the adventitia, while arteriolar endothelial cells express VEGF-C in the lungs of Sugen 5416/chronic hypoxia (SuHx) rats (*A*). VEGFR3 protein is expressed in endothelial cells in normal, chronically hypoxic, and SuHx animals and in macrophages. VEGFR3 expression is found in bronchus-associated lymphoid tissue in large and small pulmonary artery endothelial cells (*B*). Luminal endothelial cells in SuHx animals express VEGFR3 at 3 weeks of the study protocol but not any longer in the lungs of animals that had received Sugen 5416 and been exposed to chronic hypoxia and killed 6 weeks after the Sugen 5416 implantation (*C*). Asterisks indicate $P < 0.05$. $n = 4$. Hx: hypoxia-only rats.

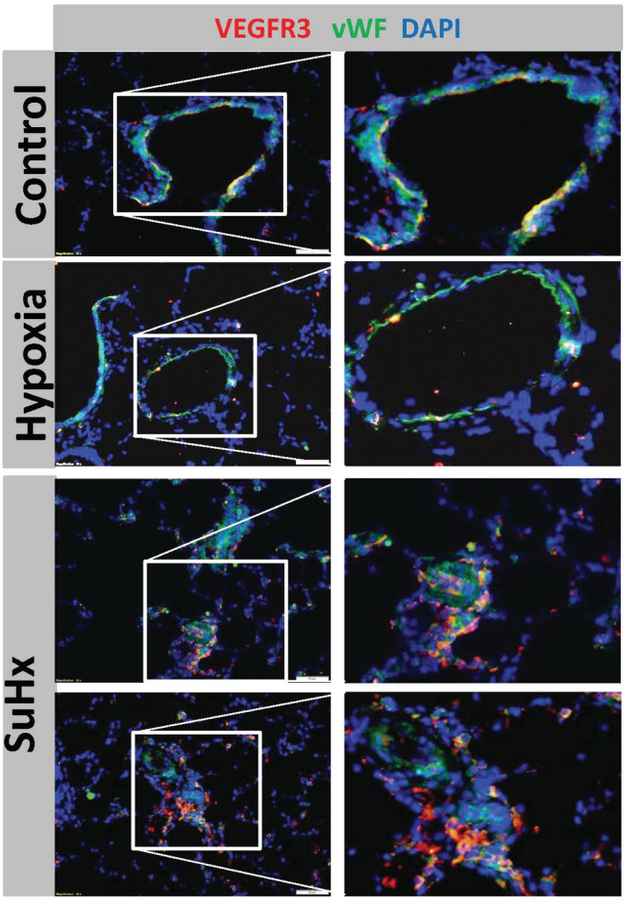

Figure 4. Double immunofluorescence staining of vascular endothelial growth factor receptor 3 (VEGFR3) and von Willebrand factor (vWF) for lung tissue sections. Control and hypoxia sections shows some of the endothelial cells of a medium vessel >50 μm expressing VEGFR3. The section from the Sugen 5416/chronic hypoxia (SuHx) rat lung shows abundant VEGFR3 expression in and around the lesion. 4′,6-Diamidino-2-phenylindole (DAPI) was used as a nuclear counterstain. Magnification, ×40.

significantly reduced (Fig. 5*D*). In addition, the amount of perivascular cell accumulation was significantly reduced, and the BALT trended toward reduction without reaching statistical significance (Fig. 5*E*, 5*F*). However, when SuHx rats with established PAH and severe right heart dysfunction were treated with the VEGFR3 inhibitor MAZ51,[32] the treatment resulted in worsening of PAH and right ventricular hypertrophy (Fig. 6*A*, 6*B*), and no changes in vascular obliteration were observed when we screened the lung sections (Fig. 6*C*), suggesting that blockade of VEGFR3 adversely affected the function of the pressure-overloaded RV.

DISCUSSION

In severe forms of angioproliferative PAH, inflammation and precursor stem cells cooperate in presently incompletely understood mechanisms to respond to endothelial cell injury and apoptosis of pulmonary microvessel cells.[6,57-60] One hypothesis attempts to address the pathobiology of lung vascular remodeling by comparing it with a quasi-neoplastic process or a process where the "vascular wound healing has gone awry."[1] Both of these concepts emphasize a disturbance of the homeostatic balance that otherwise maintains a normal pulmonary microvessel structure. One important vascular growth and maintenance factor is VEGF, as illustrated by the SuHx model of severe PAH, which depends not on gene mutations but on the actions of the antiangiogenic drug Sugen 5416. This drug inhibits the critically important VEGF-dependent growth and survival of endothelial cells, which the VEGF protein transmits predominantly via VEGFR2, Akt, and protein kinase C.[21,59] While this mechanism of drug action explains the initial endothelial cell apoptosis occurring in the SuHx rat model,[11] it does not explain the subsequent proliferation of apoptosis-resistant endothelial cells[60] or the recently described bronchus-associated lymph follicle formation.[3,4]

A recently published state-of-the-art review has discussed the SuHx model, stating that "whether VEGF inhibition promotes or inhibits PAH [is] creating confusion."[61] Unequivocally, the combination of Sugen 5416 plus chronic hypoxia in rats causes severe PAH, and a recent report now describes profound and complicated signaling changes that occur in endothelial cells as a consequence of prolonged VEGFR blockade.[17] This publication now provides a conceptual framework for the understanding of the mechanisms whereby cells can escape from antiangiogenic drug therapy.

To examine mechanisms of pulmonary microvessel proliferation following chronic hypoxic exposure combined with VEGFR1 and VEGFR2 blockade, we measured the expressed VEGF splice variants and demonstrated increased expression of the VEGFR3 protein in the lungs of SuHx rats.[62] VEGF isoforms are differentially expressed in different organs and cells. For example, the highest expression of VEGF-B is found in the developing myocardium,[36] while VEGF-C is highly expressed in lymph vessels, T lymphocytes,[63] and dendritic cells.[64] We used Western blot technology to assess the amounts of expressed proteins and thereafter IHC to identify and localize proteins in the lung tissue samples. Our data show that the isoform pattern of VEGF and the expression of VEGFR3 is altered in the lungs of SuHx rats and that treatment

of SuHx rats with the VEGFR3 inhibitor MAZ51 ameliorates the development of PAH in this model.

We recently reported increased expression of VEGFR3 and of inhibitor of differentiation 3 (ID3) in lung vascular lesions of SuHx rats and showed in cultured endothelial cells that Sugen 5416 increased expression of the transcription factors ID3, Oct-4, and Sox-2.[62] ID3 is a transcription factor that is upregulated in its expression in the pulmonary vasculature following chronic hypoxia.[65] Of interest, the experimental overexpression of ID3 in endothelial cells inhibits apoptosis and increases the expression of VEGFR3.[58] Thus, these data are consistent with the hypothesis that long-lasting Sugen 5416–triggered VEGFR1 and VEGFR2 blockade can activate in endothelial cells a stem cell–related cell proliferation mechanism[62] that includes VEGFR3 protein expression.

In the present experiments, we first assessed the tissue protein expression of the VEGF isoforms A, B, C, and D using specific antibodies and Western blotting, and we found that there is no significant change in VEGF-A and VEGF-B protein expression in the lungs of SuHx rats, while the expression of VEGF-C and VEGF-D was increased compared with that in control lungs and lungs from chronically hypoxic rats (Fig. 1). In addition, there was increased expression of the VEGFR3 protein (Fig. 1*G*).[26]

VEGFR3 is upregulated in the microvessels of tumors and wounds as well as in angiogenic sprouts, and it has been demonstrated that blockade of VEGFR3 signaling with monoclonal antibodies decreased the sprouting in angiogenic mouse models.[29] In the context of the present investigation, it is important to point out that hypoxia induces the production of VEGF-C and increases the expression of VEGFR3 in lymphatic endothelial cells.[66] VEGFR3 is expressed in macrophages[56] and is activated by binding of VEGF-C and VEGF-D. It is therefore tempting to hypothesize that the angioproliferation in the lungs of SuHx rats may also be driven by binding of the VEGF-C and VEGF-D isoform ligands to VEGFR3 and signaling through the VEGFR3. We tested this hypothesis by treating the SuHx animals with MAZ51, an inhibitor of VEGFR3 (see below).[32]

To begin the investigation of gene expression changes in the hypertensive SuHx lungs, we used microarray technology and focused on increased and decreased expression of genes encoding proteins involved in VEGF signaling and proteins that control cell growth. Interestingly, the Sugen 5416–induced VEGFR1/VEGFR2 blockade in the chronically hypoxic animals resulted in a profound downregulation of the VEGFR2 gene. To our best knowledge, this is the first time it has been shown that inhibition of the VEGFR kinase results in a downregulation of the gene encoding the VEGF receptor, suggesting a feedback mechanism between receptor function and receptor gene expression. This finding was associated with downregulation of the SPARC gene and protein.

The diminished expression of the VEGFR2 gene in combination with reduced SPARC expression are a manifestation of disturbed vascular cell homeostasis, as SPARC can act in an antiangiogenic role by affecting signaling through VEGFR2. Whether the overexpression of PLD reflects growth control signals that are routed by VEGF-C through the VEGFR3 needs further investigation. The pattern of upregulated expression of Lamp3, PLD, and eNOS and decreased expression of SPARC is characteristic of cancer cell growth and metastasis.[48,49,51,67,68]

Treating rats from the start of the SuHx protocol with MAZ51 ameliorated the developed PH and significantly reduced the number of obliterated pulmonary arterioles (Fig. 5), indicating to us that the elevated tissue levels of the isoforms VEGF-C and VEGF-D are contributing via VEGFR3 signaling to the process of lumen obliteration and perivascular inflammation. This VEGFR3-dependent mechanism is well established and has been recognized to drive lymphatic vessel growth.[69] VEGF-D serum protein levels have been measured and found to be elevated in patients with lymphangiomyomatosis,[70] but VEGF-C or VEGF-D levels have not been reported in patients with PAH.

As shown recently, the VEGFR3 inhibitor MAZ51 reduced PH in the monocrotaline model of PH.[4] The authors treated rats with MAZ51 and demonstrated a reduced resistance vessel wall thickness, reduction of RV hypertrophy, and a reduction in the mean PA pressure and in the size of BALT in a prevention trial, but apparently MAZ51 was less effective in a treatment trial. MAZ51, an indolinone that blocks the ligand-induced autophosphorylation of VEGFR3, blocks the proliferation of VEGFR3-expressing endothelial cells.[32] Although Colvin et al.[4] attributed the protective effect of MAZ51 treatment in the monocrotaline PH model to BALT size reduction and immune modulation, it is also plausible that the drug blocks the growth of VEGFR3-expressing endothelial cells, in particular in the abundant presence of the ligands VEGF-C and VEGF-D—as is the case in the SuHx model (Fig. 1*D*, 1*E*).

Intervention—that is, the treatment of SuHx rats with established PAH—had no effect on the lung vessel obliteration, suggesting that VEGFR3-signaling contributes to the development of pulmonary vascular remodeling but

Table 1. Gene expression changes in lungs of rats receiving Sugen 5416/chronic hypoxia (SuHx) treatment

Gene ID	Gene symbol	Description	Fold change (SuHx/normal)
A_44_P321009	*Cyp1a1*	*Rattus norvegicus* cytochrome P450, family 1, subfamily a, polypeptide 1 (Cyp1a1), mRNA [NM_012540]	264.507
A_44_P191778	*Cyp1b1*	*Rattus norvegicus* cytochrome P450, family 1, subfamily b, polypeptide 1 (Cyp1b1), mRNA [NM_012940]	28.697
A_44_P251228	*Cyp1b1*	*Rattus norvegicus* Sprague-Dawley cytochrome P450 (CYP1B1) mRNA, complete cds [U09540]	26.584
A_44_P304842	*Tle1_predicted*	PREDICTED: *Rattus norvegicus* transducin-like enhancer of split 1, homolog of *Drosophila* E(spl) (predicted) (Tle1_predicted), mRNA [XM_342851]	8.375
A_44_P1050510	*LOC686809*	PREDICTED: *Rattus norvegicus* similar to protein 7 transactivated by hepatitis B virus X antigen (LOC686809), mRNA [XM_001075804]	7.588
A_44_P476733	*Nqo1*	*Rattus norvegicus* NAD(P)H dehydrogenase, quinone 1 (Nqo1), mRNA [NM_017000]	5.993
A_44_P448892	*AA899841*	AA899841 UI-R-E0-cq-g-01-0-UI.s2 UI-R-E0 *Rattus norvegicus* cDNA clone UI-R-E0-cq-g-01-0-UI 3′ similar to gi [AA899841]	5.756
A_44_P1052324	*Lamp3*	*Rattus norvegicus* lysosomal-associated membrane protein 3 (Lamp3), mRNA [NM_001012015]	5.723
A_44_P323430	*Nme7*	*Rattus norvegicus* nonmetastatic cells 7, protein expressed in (Nme7), mRNA [NM_138532]	4.947
A_43_P12736	*Pld2*	*Rattus norvegicus* phospholipase D2 (Pld2), mRNA [NM_033299]	4.849
A_44_P118475	*BX883043*	*Rattus norvegicus* chromosome 20, major histocompatibility complex, assembled from 40 BACs, strain Brown Norway (BN/ssNHsd), RT1n haplotype; segment 2/11 [BX883043]	4.726
A_44_P452245	*Serpine1*	*Rattus norvegicus* serine (or cysteine) peptidase inhibitor, clade E, member 1 (Serpine1), mRNA [NM_012620]	4.356
A_44_P638176	*LOC500152*	PREDICTED: *Rattus norvegicus* similar to multimerin 1 (LOC500152), mRNA [XM_001071128]	4.205
A_44_P190088	*Prpf39_predicted*	AGENCOURT_17617267 NIH_MGC_236 *Rattus norvegicus* cDNA clone IMAGE: 7128249 5′, mRNA sequence [CK472947]	3.911
A_43_P13102	*Ada*	*Rattus norvegicus* adenosine deaminase (Ada), mRNA [NM_130399]	3.527
A_44_P233080	*Egr1*	*Rattus norvegicus* early growth response 1 (Egr1), mRNA [NM_012551]	3.502
A_44_P340236	*Clec4a1*	*Rattus norvegicus* C-type lectin domain family 4, member a1 (Clec4a1), mRNA [NM_001005890]	3.438
A_44_P905727	*TC628605*	Q9D6B0_MOUSE (Q9D6B0) 18 days pregnant adult female placenta and extra embryonic tissue cDNA, RIKEN full-length enriched library, clone: 3830420G05, product: G protein–coupled receptor 97, full insert sequence, partial (13%) [TC628605]	3.367
A_44_P100565	*A_44_P100565*	Unknown	3.163
A_44_P368134	*Sncaip_predicted*	PREDICTED: *Rattus norvegicus* synuclein, alpha interacting protein (synphilin) (predicted) (Sncaip_predicted), mRNA [XM_225768]	3.121
A_44_P570604	*DN932947*	AGENCOURT_50134677 NCI_CGAP_Pr49 *Rattus norvegicus* cDNA clone IMAGE: 7930540 5′, mRNA sequence [DN932947]	3.100
A_44_P279452	*AA957814*	UI-R-E1-fz-b-03-0-UI.s1 UI-R-E1 *Rattus norvegicus* cDNA clone UI-R-E1-fz-b-03-0-UI 3′, mRNA sequence [AA957814]	2.982
A_44_P198620	*Nos3*	*Rattus norvegicus* nitric oxide synthase 3, endothelial cell (Nos3), mRNA [NM_021838]	2.624
A_42_P538400	*Ntrk2*	*Rattus norvegicus* neurotrophic tyrosine kinase, receptor, type 2 (Ntrk2), mRNA [NM_012731]	2.595
A_42_P812263	*Sat*	*Rattus norvegicus* spermidine/spermine N1-acetyl transferase (Sat), mRNA [NM_001007667]	2.586

Table 1 (*continued*)

Gene ID	Gene symbol	Description	Fold change (SuHx/normal)
A_43_P11686	*Kdr*	*Rattus norvegicus* kinase insert domain protein receptor (Kdr), mRNA [NM_013062]	0.155
A_44_P778356	*Hey2*	PREDICTED: *Rattus norvegicus* hairy [XM_344806]	0.174
A_44_P120219	*AI177943*	AI177943 EST221594 Normalized rat placenta, Bento Soares *Rattus* sp. cDNA clone RPLCI92 3′ end, mRNA sequence [AI177943]	0.191
A_44_P527947	*AA925093*	UI-R-A1-ei-a-08-0-UI.s1 UI-R-A1 *Rattus norvegicus* cDNA clone UI-R-A1-ei-a-08-0-UI 3′, mRNA sequence [AA925093]	0.199
A_44_P292689	*Syt1*	*Rattus norvegicus* partial mRNA for synaptotagmin 1 (syt1 gene), splice variant 4 [AJ617619]	0.237
A_42_P817086	*Scnn1b*	*Rattus norvegicus* sodium channel, nonvoltage-gated 1 beta (Scnn1b), mRNA [NM_012648]	0.251
A_42_P683634	*Sparcl1*	*Rattus norvegicus* SPARC-like 1 (mast9, hevin) (Sparcl1), mRNA [NM_012946]	0.260
A_44_P181094	*AI600081*	EST251784 Normalized rat embryo, Bento Soares *Rattus* sp. cDNA clone REMDQ91 3′ end, mRNA sequence [AI600081]	0.295
A_44_P718743	*TC648865*	Unknown	0.298
A_44_P375102	*XM_214014*	*Rattus norvegicus* similar to mac25 (LOC289560), mRNA [XM_214014]	0.318
A_44_P240274	*Emcn*	*Rattus norvegicus* endomucin (Emcn), mRNA [NM_001004228]	0.328
A_44_P752342	*BF563060*	UI-R-BO1-aiy-b-03-0-UI.r1 UI-R-BO1 *Rattus norvegicus* cDNA clone UI-R-BO1-aiy-b-03-0-UI 5′, mRNA sequence [BF563060]	0.344
A_44_P206985	*Gnrh1*	*Rattus norvegicus* gonadotropin-releasing hormone 1 (Gnrh1), mRNA [NM_012767]	0.346
A_44_P123492	*Epb4.1l3*	*Rattus norvegicus* erythrocyte protein band 4.1–like 3 (Epb4.1l3), mRNA [NM_053927]	0.350
A_42_P556829	*Wif1*	*Rattus norvegicus* Wnt inhibitory factor 1 (Wif1), mRNA [NM_053738]	0.354
A_44_P229118	*Muc1*	Mucin 1 (fragment) [Source: Uniprot/SPTREMBL; Acc: O35770] [ENSRNOT00000027850]	0.359
A_44_P405071	*Cdk6*	Cyclin-dependent kinase 6 (fragment) [Source: Uniprot/SPTREMBL; Acc: Q99MD0] [ENSRNOT00000012597]	0.363
A_44_P937141	*AW917120*	AW917120 EST348424 Rat gene index, normalized rat, norvegicus, Bento Soares *Rattus norvegicus* cDNA clone RGIDZ48 5′ end, mRNA sequence [AW917120]	0.388
A_44_P607972	*TC593692*	Unknown	0.398
A_44_P962361	*TC608677*	Unknown	0.430
A_43_P12613	*Apln*	*Rattus norvegicus* apelin, AGTRL1 ligand (Apln), mRNA [NM_031612]	0.459
A_42_P806859	*AI229721*	AI229721 EST226416 Normalized rat embryo, Bento Soares *Rattus* sp. cDNA clone REMCL08 3′ end, mRNA sequence [AI229721]	0.465
A_42_P469969	*Igsf10*	*Rattus norvegicus* immunoglobulin superfamily, member 10 (Igsf10), mRNA [NM_198768]	0.482
A_44_P983155	*LOC292209*	PREDICTED: *Rattus norvegicus* similar to GTPase activating protein testicular GAP1 (LOC292209), mRNA [XM_238066]	0.487
A_44_P409975	*Wee1*	*Rattus norvegicus* wee1 homolog (*S. pombe*) (Wee1), mRNA [NM_001012742]	0.496

Note: Validation of gene expression changes is shown for 90 genes demonstrated by quantitative polymerase chain reaction (PCR) analysis using the SABiosciences VEGF Signaling PCR Array. Those genes with statistically significant differences between normal and SuHx lungs are given here ($n = 2$, $P < 0.05$, t test). The average fold change (SuHx/normal) is shown for the most differentially expressed genes.

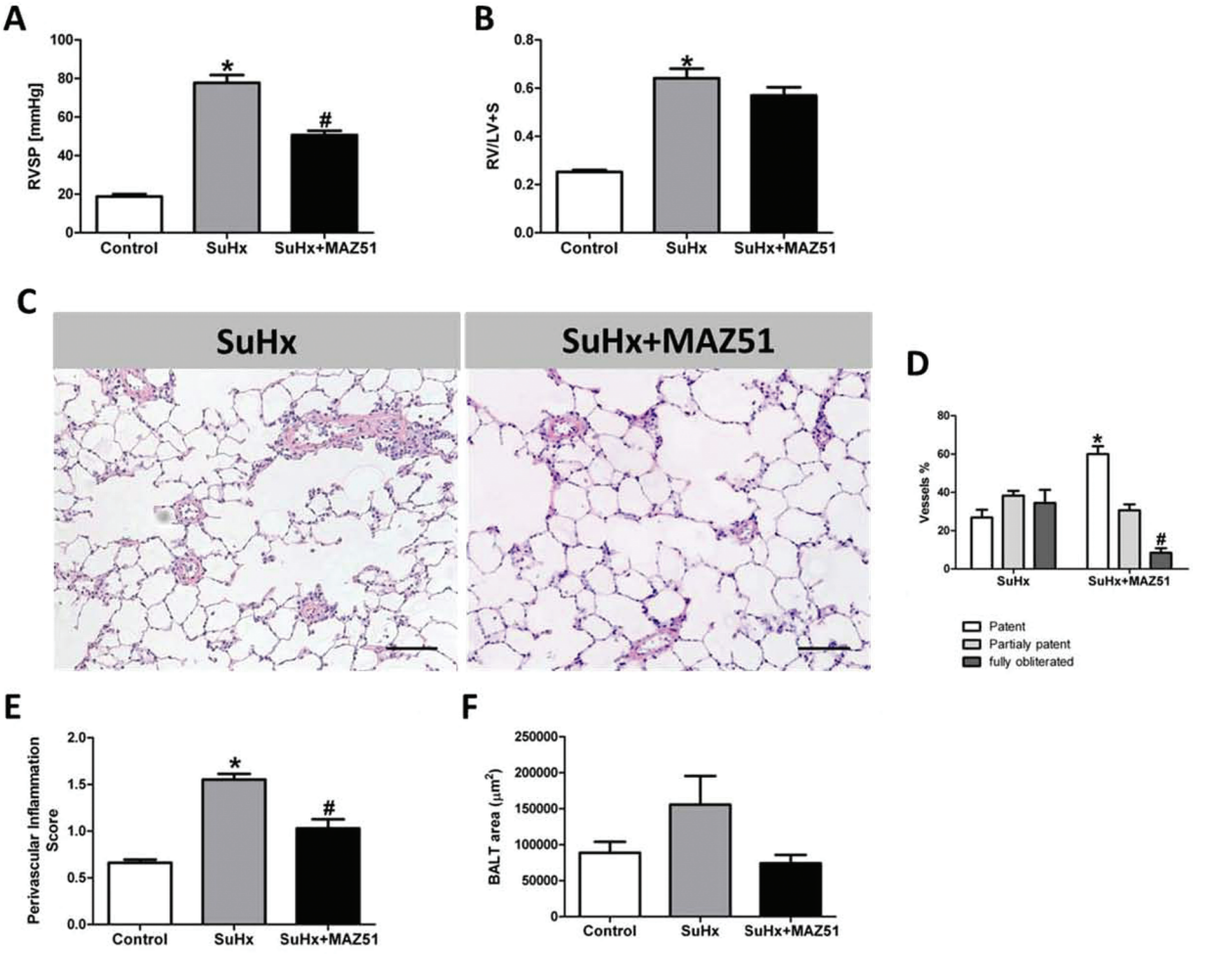

Figure 5. Concomitant treatment of Sugen 5416/chronic hypoxia (SuHx) rats with the vascular endothelial growth factor receptor 3 (VEGFR3) blocker MAZ51 reduced right ventricular systolic pressure (RVSP; *A*), the number of obliterated lung arterioles (*C–D*), the degree of perivascular cell accumulation (*E*), and the size of the bronchoalveolar lymph cell aggregate (*F*). Asterisks indicate $P < 0.05$. $n = (4–7)$. Magnification, ×10. Scale = 50 μm. RV/LV+S: ratio of right ventricular weight to left ventricular plus septal weight; BALT: bronchus-associated lymphoid tissue.

that the lesions, when established, cannot be reversed by VEGFR3 blockade. Whether the worsening of RVSP by MAZ51 treatment of established PAH points toward a supportive role of VEGFR3 signaling in the failing heart is unclear. Whereas we cannot find any publication reporting on VEGFR3 signaling in the heart, our data show a dramatic reduction in VEGF-D and VEGF-B ligands expression in the failing SuHx rat RV and a trend toward reduced expression of VEGF-C (Fig. 2*C*–2*E*). Hagberg et al.[71] have reported that VEGF-B controls endothelial cell fatty acid uptake, and Serpi et al.[72] showed that VEGF-B increased the growth of capillaries in rat left ventricles. Our present finding of reduced VEGF-B expression in the failing SuHx rat RVs complement previously published data that show a multilevel impairment of fatty acid oxidation in the SuHx RV tissues.[34] Indeed, reduced fatty acid transport across cardiac endothelial cells, as a consequence of reduced VEGF-B expression, can perhaps be an indicator of impaired myocardial endothelial cell function in the failing RV. While the homeostatic role of VEGF-A in the myocardium has been well established[39] and inhibition of VEGF signaling has been shown to trigger myocardial hibernation,[39] upregulation of the expression of soluble growth factor receptor 1 (sVEGFR1 or sFlt-1) has been shown to prevent angiogenesis in the hypertrophied myocardium.[73] We found that the sFlt-1 protein concentration in the serum and RV tissues trended toward being increased in SuHx rats (Figs. 1*I*, 2*G*). Thus,

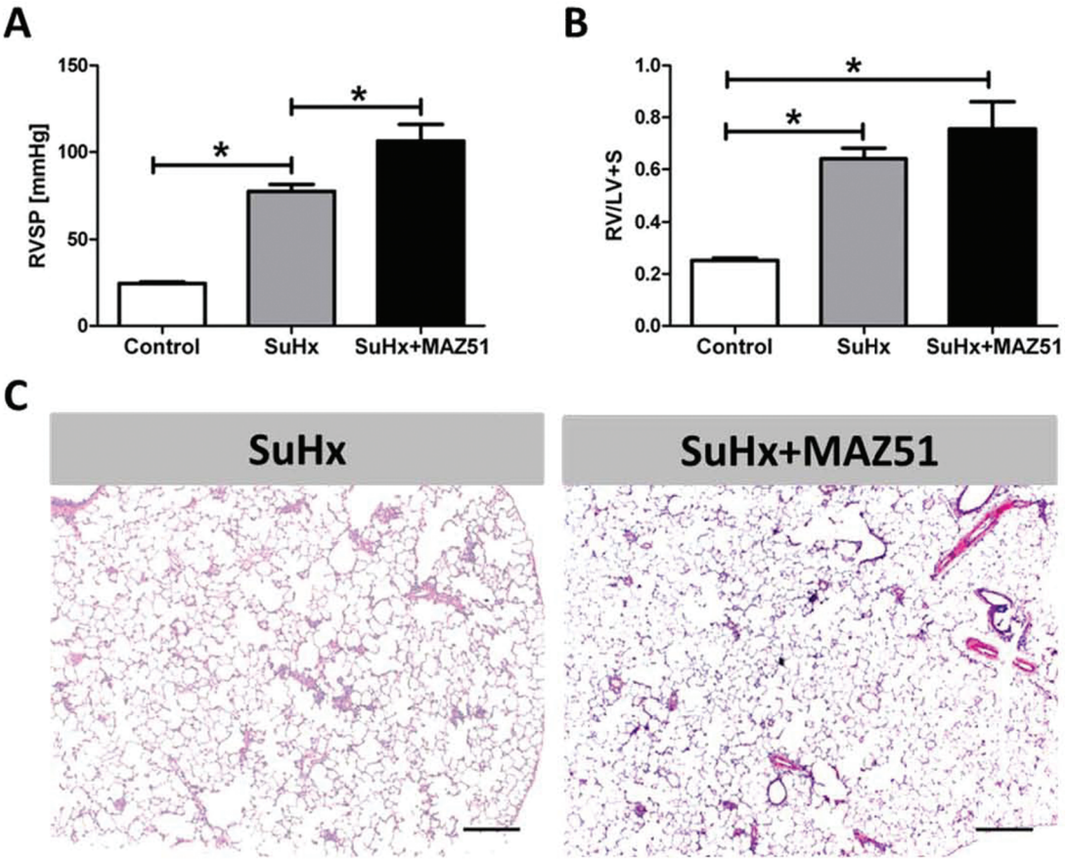

Figure 6. Treatment of animals with established Sugen 5416/chronic hypoxia (SuHx)–triggered pulmonary hypertension with the vascular endothelial growth factor receptor 3 (VEGFR3) inhibitor MAZ51 for 2 weeks worsened the degree of pulmonary hypertension when assessed by measurement of right ventricular systolic pressure (RVSP; *A*). In addition to the persistence of small arteriole occlusion, the vessels appear highly muscularized (*C*). Asterisks indicate $P < 0.05$. $n = 3$. Magnification, ×2.5. Scale = 100 μm.

the decreased expression of the ligand proteins VEGF-A,[35] VEGF-B, and perhaps VEGF-D and VEGF-C, together with high circulating levels of the antiangiogenic sFlt-1, could all account for the capillary rarefaction of the failing SuHx rat RV and the metabolic remodeling of the RV tissue.[34] Table 2 lists the RV and lung tissue VEGF isoform expression changes.

To summarize, the paradox that treatment of hypoxic rats with the antiangiogenic VEGFR kinase blocker Sugen 5416 induces angioproliferation and lung vessel lumen obliteration can in part be explained by a change in the VEGF isoform ligand expression pattern and signaling via VEGFR3. Both VEGF-C and VEGF-D could activate VEGFR3 and cause endothelial cell proliferation.

This conclusion is supported by our data that demonstrate that blockade of VEGFR3, due to treatment of rats with MAZ51, largely prevents pulmonary angiooblitera-tion and perivascular cell infiltration in the SuHx model of severe PAH, while treatment of animals with established pulmonary vascular lesions with MAZ51 does not reopen vascular lesions but instead worsens the degree of PAH and RV hypertrophy.

We emphasize that the roles of sFlt-1 in this model need further investigation, in particular in view of the reported high serum sFlt-1 levels in patients with IPAH.[74]

The second paradox that characterizes the SuHx rat model is that the proliferative lung microangiopathy is paired with the antiangiogenic environment of the failing RV.

Finally and again paradoxically, VEGF inhibition may in the lungs both initiate endothelial cell apoptosis and subsequently facilitate angiooblitération. We speculate that in human forms of severe angiooblitérative PAH endogenous antiangiogenic factors like sFlt-1 and endoglin[70]

Table 2. Right ventricle (RV) and lung tissue vascular endothelial growth factor (VEGF) isoform expression changes

	SuHx vs. control	
	Lung tissue	RV tissue
VEGF-A	→	↓↓
VEGF-B	→	↓
VEGF-C	↑↑	↓
VEGF-D	↑↑	↓
VEGFR2	→	NA
VEGFR3	↑↑	NA

Note: Shown are VEGF isoform and VEGF receptor protein expression changes in Sugen 5416/chronic hypoxia (SuHx) lungs and right ventricle tissue compared with controls. NA: not available.

may cause the initial endothelial cell death by inhibiting VEGF-dependent cell survival and that VEGFR3-expressing stem or progenitor cells[62] may grow when the receptor is activated by VEGF-C and/or VEGF-D.

Source of Support: This work was supported by funds from the Victoria Johnson Center for Obstructive Lung Research.

Conflict of Interest: None declared.

REFERENCES

1. Voelkel NF, Gomez-Arroyo J, Abbate A, Bogaard HJ, Nicolls MR. Pathobiology of pulmonary arterial hypertension and right ventricular failure. Eur Respir J 2012;40(6):1555–1565.
2. Hassoun PM, Mouthon L, Barbera JA, Eddahibi S, Flores SC, Grimminger F, et al. Inflammation, growth factors, and pulmonary vascular remodeling. J Am Coll Cardiol 2009;54 (suppl):S10–S19.
3. Perros F, Dorfmuller P, Montani D, Hammad H, Waelput W, Girerd B, et al. Pulmonary lymphoid neogenesis in idiopathic pulmonary arterial hypertension. Am J Respir Crit Care Med 2012;185(3):311–321.
4. Colvin KL, Cripe PJ, Ivy DD, Stenmark KR, Yeager ME. Bronchus-associated lymphoid tissue in pulmonary hypertension produces pathologic autoantibodies. Am J Respir Crit Care Med 2013;188(9):1126–1136.
5. Tian W, Jiang X, Tamosiuniene R, Sung YK, Qian J, Dhillon G, et al. Blocking macrophage leukotriene B_4 prevents endothelial injury and reverses pulmonary hypertension. Sci Transl Med 2013;5(200):200ra117.
6. Chow K, Fessel JP, Ihida-Stansbury K, Schmidt EP, Gaskill C, Alvarez D, et al. Dysfunctional resident lung mesenchymal stem cells contribute to pulmonary microvascular remodeling. Pulm Circ 2013;3(1):31–49.
7. Rabinovitch M. Molecular pathogenesis of pulmonary arterial hypertension. J Clin Invest 2012;122(12):4306–4313.
8. Spiekerkoetter E, Tian X, Cai J, Hopper RK, Sudheendra D, Li CG, et al. FK506 activates BMPR2, rescues endothelial dysfunction, and reverses pulmonary hypertension. J Clin Invest 2013;123(8):3600–3613.
9. Taraseviciene-Stewart L, Gera L, Hirth P, Voelkel NF, Tuder RM, Stewart JM. A bradykinin antagonist and a caspase inhibitor prevent severe pulmonary hypertension in a rat model. Can J Physiol Pharmacol 2002;80(4):269–274.
10. Abe K, Toba M, Alzoubi A, Ito M, Fagan KA, Cool CD, et al. Formation of plexiform lesions in experimental severe pulmonary arterial hypertension. Circulation 2010;121(25):2747–2754.
11. Taraseviciene-Stewart L, Kasahara Y, Alger L, Hirth P, McMahon G, Waltenberger J, et al. Inhibition of the VEGF receptor 2 combined with chronic hypoxia causes cell death–dependent pulmonary endothelial cell proliferation and severe pulmonary hypertension. FASEB J 2001;15(2):427–438.
12. Meloche J, Courchesne A, Barrier M, Carter S, Bisserier M, Paulin R, et al. Critical role for the advanced glycation endproducts receptor in pulmonary arterial hypertension etiology. J Am Heart Assoc 2013;2(1):e005157.
13. De Bock K, Georgiadou M, Carmeliet P. Role of endothelial cell metabolism in vessel sprouting. Cell Metab 2013;18 (5):634–647.
14. Benedito R, Rocha SF, Woeste M, Zamykal M, Radtke F, Casanovas O, et al. Notch-dependent VEGFR3 upregulation allows angiogenesis without VEGF-VEGFR2 signalling. Nature 2012;484(7392):110–114.
15. Arany Z, Foo S-Y, Ma Y, Ruas JL, Bommi-Reddy A, Girnun G, et al. HIF-independent regulation of VEGF and angiogenesis by the transcriptional coactivator PGC-1α. Nature 2008;451(7181):1008–1012.
16. Mountzios G, Pentheroudakis G, Carmeliet P. Bevacizumab and micrometastases: revisiting the preclinical and clinical rollercoaster. Pharmacol Ther 2014;141(2):117–124.
17. Zhuang G, Yu K, Jiang Z, Chung A, Yao J, Ha C, et al. Phosphoproteomic analysis implicates the mTORC2-FoxO1 axis in VEGF signaling and feedback activation of receptor tyrosine kinases. Sci Signal 2013;6(271):ra25.
18. Sennino B, McDonald DM. Controlling escape from angiogenesis inhibitors. Nat Rev Cancer 2012;12(10):699–709.
19. Gupta K, Kshirsagar S, Li W, Gui L, Ramakrishnan S, Gupta P, et al. VEGF prevents apoptosis of human microvascular endothelial cells via opposing effects on MAPK/ERK and SAPK/JNK signaling. Exp Cell Res 1999;247(2):495–504.
20. Carmeliet P. Mechanisms of angiogenesis and arteriogenesis. Nat Med 2000;6(4):389–395.
21. Chen J, Somanath PR, Razorenova O, Chen WS, Hay N, Bornstein P, et al. Akt1 regulates pathological angiogenesis, vascular maturation and permeability in vivo. Nat Med 2005;11(11):1188–1196.
22. Gavard J, Gutkind JS. VEGF controls endothelial-cell permeability by promoting the β-arrestin-dependent endocytosis of VE-cadherin. Nat Cell Biol 2006;8(11):1223–1234.
23. Koch S, Claesson-Welsh L. Signal transduction by vascular endothelial growth factor receptors. Cold Spring Harb Perspect Med 2012;2(7):a006502.

24. Domingues I, Rino J, Demmers JA, de Lanerolle P, Santos SC. VEGFR2 translocates to the nucleus to regulate its own transcription. PLoS ONE 2011;6(9):e25668.
25. Tuder RM, Chacon M, Alger L, Wang J, Taraseviciene-Stewart L, Kasahara Y, et al. Expression of angiogenesis-related molecules in plexiform lesions in severe pulmonary hypertension: evidence for a process of disordered angiogenesis. J Pathol 2001;195(3):367–374.
26. Hewett PW, Murray JC. Coexpression of *flt*-1, *flt*-4 and *KDR* in freshly isolated and cultured human endothelial cells. Biochem Biophys Res Commun 1996;221(3):697–702.
27. Ristimaki A, Narko K, Enholm B, Joukov V, Alitalo K. Proinflammatory cytokines regulate expression of the lymphatic endothelial mitogen vascular endothelial growth factor–C. J Biol Chem 1998;273(14):8413–8418.
28. Janer J, Lassus P, Haglund C, Paavonen K, Alitalo K, Andersson S. Pulmonary vascular endothelial growth factor–C in development and lung injury in preterm infants. Am J Respir Crit Care Med 2006;174(3):326–330.
29. Tammela T, Zarkada G, Wallgard E, Murtomaki A, Suchting S, Wirzenius M, et al. Blocking VEGFR-3 suppresses angiogenic sprouting and vascular network formation. Nature 2008;454(7204):656–660.
30. Datar SA, Johnson EG, Oishi PE, Johengen M, Tang E, Aramburo A, et al. Altered lymphatics in an ovine model of congenital heart disease with increased pulmonary blood flow. Am J Physiol Lung Cell Mol Physiol 2012;302(6):L530–L540.
31. Bahram F, Claesson-Welsh L. VEGF-mediated signal transduction in lymphatic endothelial cells. Pathophysiology 2010; 17(4):253–261.
32. Kirkin V, Thiele W, Baumann P, Mazitschek R, Rohde K, Fellbrich G, et al. MAZ51, an indolinone that inhibits endothelial cell and tumor cell growth in vitro, suppresses tumor growth in vivo. Int J Cancer 2004;112(6):986–993.
33. Lin CI, Chen CN, Huang MT, Lee SJ, Lin CH, Chang CC, et al. Lysophosphatidic acid up-regulates vascular endothelial growth factor–C and lymphatic marker expressions in human endothelial cells. Cell Mol Life Sci 2008;65(17):2740–2751.
34. Gomez-Arroyo J, Szczepanek K, Syed A, Farkas L, Farkas D, Kraskauskas D, et al. Metabolic remodeling in right heart failure is associated with abnormal mitochondrial biogenesis. Am J Respir Crit Care Med 2012;185:A3455.
35. Bogaard HJ, Natarajan R, Mizuno S, Abbate A, Chang PJ, hau VQ, et al. Adrenergic receptor blockade reverses right heart remodeling and dysfunction in pulmonary hypertensive rats. Am J Respir Crit Care Med 2010:182(5):652–660.
36. Olofsson B, Pajusola K, Kaipainen A, von Euler G, Joukov V, Saksela O, et al. Vascular endothelial growth factor B, a novel growth factor for endothelial cells. Proc Natl Acad Sci USA 1996;93(6):2576–2581.
37. Olofsson B, Korpelainen E, Pepper MS, Mandriota SJ, Aase K, Kumar V, et al. Vascular endothelial growth factor B (VEGF-B) binds to VEGF receptor–1 and regulates plasminogen activator activity in endothelial cells. Proc Natl Acad Sci USA 1998;95(20):11709–11714.
38. Bry M, Kivela R, Holopainen T, Anisimov A, Tammela T, Soronen J, et al. Vascular endothelial growth factor–B acts as a coronary growth factor in transgenic rats without inducing angiogenesis, vascular leak, or inflammation. Circulation 2010;122(17):1725–1733.
39. May D, Gilon D, Djonov V, Itin A, Lazarus A, Gordon O, et al. Transgenic system for conditional induction and rescue of chronic myocardial hibernation provides insights into genomic programs of hibernation. Proc Natl Acad Sci USA 2008;105(1):282–287.
40. Stacher E, Graham BB, Hunt JM, Gandjeva A, Groshong SD, McLaughlin VV, et al. Modern age pathology of pulmonary arterial hypertension. Am J Respir Crit Care Med 2012;186(3):261–272.
41. Yee HY, Paquet A, Dudoit S. Exploratory analysis for two-color spotted microarray data. R package version 1.20.0, 2007.
42. Simon R, Korn E, McShane L, Radmacher M, Wright G, Zhao Y. Design and analysis of DNA microarray investigations. New York: Springer, 2003.
43. Tusher VG, Tibshirani R, Chu G. Significance analysis of microarrays applied to the ionizing radiation response. Proc Natl Acad Sci USA 2001;98:5116–5121.
44. Al Husseini A, Wijesinghe DS, Farkas A, Kraskauskas D, Drake J, Chalfant CE, et al. Increased eicosanoid levels in the Sugen/chronic hypoxia model of severe pulmonary hypertension. Am J Respir Crit Care Med 2013;187:A4631.
45. Drake JI, Bogaard HJ, Mizuno S, Clifton B, Xie B, Gao Y, et al. Molecular signature of a right heart failure program in chronic severe pulmonary hypertension. Am J Respir Cell Mol Biol 2011;45(6):1239–1247.
46. Seymour LW, Shoaibi MA, Martin A, Ahmed A, Elvin P, Kerr DJ, et al. Vascular endothelial growth factor stimulates protein kinase C–dependent phospholipase D activity in endothelial cells. Lab Invest 1996;75(3):427–437.
47. Cho CH, Lee CS, Chang M, Jang IH, Kim SJ, Hwang I, et al. Localization of VEGFR-2 and PLD2 in endothelial caveolae is involved in VEGF-induced phosphorylation of MEK and ERK. Am J Physiol Heart Circ Physiol 2004;286(5):H1881–H1888.
48. Ozaki K, Nagata M, Suzuki M, Fujiwara T, Ueda K, Miyoshi Y, et al. Isolation and characterization of a novel human lung–specific gene homologous to lysosomal membrane glycoproteins 1 and 2: significantly increased expression in cancers of various tissues. Cancer Res 1998;58(16):3499–3503.
49. Kanao H, Enomoto T, Kimura T, Fujita M, Nakashima R, Ueda Y, et al. Overexpression of LAMP3/TSC403/DC-LAMP promotes metastasis in uterine cervical cancer. Cancer Res 2005;65(19):8640–8645.
50. Kobayashi T, Vischer UM, Rosnoblet C, Lebrand C, Lindsay M, Parton RG, et al. The tetraspanin CD63/lamp3 cycles between endocytic and secretory compartments in human endothelial cells. Mol Biol Cell 2000;11(5):1829–1843.
51. Nagelkerke A, Mujcic H, Bussink J, Wouters BG, van Laarhoven HW, Sweep FC, et al. Hypoxic regulation and prognostic value of LAMP3 expression in breast cancer. Cancer 2011;117(16):3670–3681.
52. Kupprion C, Motamed K, Sage EH. SPARC (BM-40, osteonectin) inhibits the mitogenic effect of vascular endothelial growth factor on microvascular endothelial cells. J Biol Chem 1998;273(45):29635–29640.
53. Chandrasekaran V, Ambati J, Ambati BK, Taylor EW. Molecular docking and analysis of interactions between vas-

cular endothelial growth factor (VEGF) and SPARC protein. J Mol Graph Model 2007;26(4):775–782.
54. Nozaki M, Sakurai E, Raisler BJ, Baffi JZ, Witta J, Ogura Y, et al. Loss of SPARC-mediated VEGFR-1 suppression after injury reveals a novel antiangiogenic activity of VEGF-A. J Clin Invest 2006;116(2):422–429.
55. Kato Y, Lewalle JM, Baba Y, Tsukuda M, Sakai N, Baba M, et al. Induction of SPARC by VEGF in human vascular endothelial cells. Biochem Biophys Res Commun 2001;287 (2):422–426.
56. Rivera LB, Bradshaw AD, Brekken RA. The regulatory function of SPARC in vascular biology. Cell Mol Life Sci 2011;68 (19):3165–3173.
57. Archer SL, Weir EK, Wilkins MR. Basic science of pulmonary arterial hypertension for clinicians: new concepts and experimental therapies. Circulation 2010;121(18):2045–2066.
58. Lee C, Mitsialis SA, Aslam M, Vitali SH, Vergadi E, Konstantinou G, et al. Exosomes mediate the cytoprotective action of mesenchymal stromal cells on hypoxia-induced pulmonary hypertension. Circulation 2012;126(22):2601–2611.
59. Wu LW, Mayo LD, Dunbar JD, Kessler KM, Baerwald MR, Jaffe EA, et al. Utilization of distinct signaling pathways by receptors for vascular endothelial cell growth factor and other mitogens in the induction of endothelial cell proliferation. J Biol Chem 2000;275(7):5096–5103.
60. Sakao S, Taraseviciene-Stewart L, Cool CD, Tada Y, Kasahara Y, Kurosu K, et al. VEGF-R blockade causes endothelial cell apoptosis, expansion of surviving $CD34^{+}$ precursor cells and transdifferentiation to smooth muscle-like and neuronal-like cells. FASEB J 2007;21(13):3640–3652.
61. Sutendra G, Michelakis ED. Pulmonary arterial hypertension: challenges in translational research and a vision for change. Sci Transl Med 2013;5(208):208sr5.
62. Das JK, Voelkel NF, Felty Q. Overexpression of ID3 promotes a stem-like molecular signature in human endothelial cells: it's implications in the development of hyperproliferative endothelial lesions associated with pulmonary hypertension. Pulm Circ (forthcoming).
63. Leclers D, Durand K, Cook-Moreau J, Rabinovitch-Chable H, Sturtz FG, Rigaud M. VEGFR-3, VEGF-C and VEGF-D mRNA quantification by RT-PCR in different human cell types. Anticancer Res 2006;26(3A):1885–1891.
64. Chen L, Hamrah P, Cursiefen C, Zhang Q, Pytowski B, Streilein JW, et al. Vascular endothelial growth factor receptor–3 mediates induction of corneal alloimmunity. Nat Med 2004;10(8):813–815.
65. Yang J, Li X, Li Y, Southwood M, Ye L, Long L, et al. Id proteins are critical downstream effectors of BMP signaling in human pulmonary arterial smooth muscle cells. Am J Physiol Lung Cell Mol Physiol 2013;305(4):L312–L321.
66. Min Y, Ghose S, Boelte K, Li J, Yang L, Lin PC. C/EBP-δ regulates VEGF-C autocrine signaling in lymphangiogenesis and metastasis of lung cancer through HIF-1α. Oncogene 2011;30(49):4901–4909.
67. Zhang JL, Chen GW, Liu YC, Wang PY, Wang X, Wan YL, et al. Secreted protein acidic and rich in cysteine (SPARC) suppresses angiogenesis by down-regulating the expression of VEGF and MMP-7 in gastric cancer. PloS ONE 2012;7 (9):e44618.
68. Gomez-Cambronero J. Phosphatidic acid, phospholipase D and tumorigenesis. Adv Biol Regul 2014;54:197–206.
69. Alitalo K. The lymphatic vasculature in disease. Nat Med 2011;17(11):1371–1380.
70. Young LR, Inoue Y, McCormack FX. Diagnostic potential of serum VEGF-D for lymphangioleiomyomatosis. N Engl J Med 2008;358(2):199–200.
71. Hagberg CE, Falkevall A, Wang X, Larsson E, Huusko J, Nilsson I, et al. Vascular endothelial growth factor B controls endothelial fatty acid uptake. Nature 2010;464(7290): 917–921.
72. Serpi R, Tolonen AM, Huusko J, Rysa J, Tenhunen O, Yla-Herttuala S, et al. Vascular endothelial growth factor–B gene transfer prevents angiotensin II–induced diastolic dysfunction via proliferation and capillary dilatation in rats. Cardiovasc Res 2011;89(1):204–213.
73. Kaza E, Ablasser K, Poutias D, Griffiths ER, Saad FA, Hofstaetter JG, et al. Up-regulation of soluble vascular endothelial growth factor receptor–1 prevents angiogenesis in hypertrophied myocardium. Cardiovasc Res 2011;89(2):410–418.
74. Malhotra R, Paskin-Flerlage S, Zamanian RT, Zimmerman P, Schmidt JW, Deng DY, et al. Circulating angiogenic modulatory factors predict survival and functional class in pulmonary arterial hypertension. Pulm Circ 2013;3(2): 369–380.